Research Article

PLX8394, a RAF inhibitor, inhibits enterovirus 71 replication by blocking RAF/MEK/ERK signaling

Chengyuan Wu [a,1], Guangyan Zhu [a,1], Fang Qiu [a], Fuli Ren [a,b], Binbin Lin [a,c], Dingyu Zhang [a,*], Qingyu Yang [a,*], Chaolin Huang [a,*]

[a] Wuhan Jinyintan Hospital, Tongji Medical College of Huazhong University of Science and Technology, Wuhan, 430023, China
[b] State Key Laboratory of Virology, Wuhan Institute of Virology, Chinese Academy of Sciences, Wuhan, 430071, China
[c] Division of Life Sciences and Medicine, University of Science and Technology of China, Hefei, 230027, China

ABSTRACT

Enterovirus 71 (EV71) poses a serious threat to human health, with scattered outbreaks worldwide. There are several vaccines against a few EV71 strains but no efficient drug for the treatment of EV71 infection. Therefore, it is urgent and of significance to develop anti-EV71 drugs. Here, we found that PLX8394, a RAF inhibitor, possesses high antiviral activity against EV71 *in vitro*, being superior to the traditional clinical drug ribavirin. Moreover, PLX8394 exhibits broad-spectrum antiviral activity against enteroviruses. Notably, in a suckling mouse model, PLX8394 provided a 70% protection rate for EV71-infected mice, reduced the viral load in liver and heart tissues, and relieved the inflammatory response. A mechanistic study showed that PLX8394 inhibited EV71 by suppressing the RAF/MEK/ERK signaling pathway. Thus, PLX8394 lays a foundation for the development of new drugs against EV71.

1. Introduction

Enterovirus 71 (EV71) is a member of the *Picornaviridae* genus belonging to positive single-stranded RNA viruses that causes various clinical diseases, including hand, foot, and mouth disease, pharyngitis, enteritis, and herpangina, and severe neurological complications, such as encephalitis, cardiopulmonary failure, and neurogenic pulmonary edema, which can even lead to death (Chang et al., 2004). Since EV71 was first isolated in California in 1969, it has caused multiple outbreaks and spread around the world. The largest outbreak occurred in the Asia-Pacific region in 2008, with numerous reported cases of central nervous system complications and deaths (Schmidt et al., 1974; Han et al., 2020), indicating that EV71 poses a global public health threat (Yip et al., 2013). Several types of vaccines have been developed; however, no specific drugs against EV71 have been approved (Chong et al., 2015; Yee and Laa Poh, 2017). This highlights the urgent need to develop an effective antiviral drug for the treatment of EV71 infection.

Viruses rely on the host cell environment for replication. They can hijack cellular signaling pathways to facilitate their replication (Nagata et al., 2008; Xu et al., 2020). Therefore, virus-supportive cellular signaling pathways may be promising novel antiviral targets (Ludwig et al., 2003; Ludwig, 2011; Pei et al., 2022). Moreover, host-targeting antiviral drugs are less prone to developing drug resistance, especially for highly mutative RNA viruses (Ji and Li, 2020). Among the numerous cellular signaling pathways hijacked by EV71, the mitogen-activated protein kinase (MAPK) signaling pathway is related to the regulation of cell growth, cell development, differentiation, stress-induced apoptosis, and inflammation (Bogoyevitch and Kobe, 2006; Bian et al., 2015; Leong et al., 2015). Peng et al. (2014) demonstrated that MAPK, JNK1/2, and P38 promoted EV71 replication while their inhibitors SP600125 and SB203580 inhibited viral replication. The RAF/MEK/ERK signaling pathway belongs to the classical MAPK cascades and plays important roles in cell growth and development. The RAF family includes A-RAF, B-RAF, and C-RAF, which are serine/threonine protein kinases and can form RAF homo or hetero dimers, activating the downstream MEK1/2 protein via a process called phosphorylation; MEK kinases activate the downstream ERK1/2 through MEK phosphorylation (Dai et al., 2021). Zhang et al. (2014) reported that the overexpression of miR-27a inhibited EV71 replication by suppressing the phosphorylation of Akt and ERK. Therefore, the RAF/MEK/ERK pathway may be a promising novel antiviral target.

PLX8394 is a new RAF inhibitor that selectively inhibits B-RAF:C-RAF heterodimerization. It interacts with amino acid residues R506/K507 in B-RAF and R398/K399 in C-RAF and is used to treat tumors with activated B-RAF mutants or fusions (Yao et al., 2019; Khojasteh Poor et al., 2021). In this study, we reported for the first time, the antiviral effect of PLX8394 against EV71 and other enteroviruses using *in vitro* and *in vivo* assays.

2. Materials and methods

2.1. Cells, viruses, compounds, and antibodies

Human rhabdomyosarcoma cells (RD cells), Henrietta Lacks cells (HeLa cells), and African green monkey kidney cells (Vero cells) were cultured in Dulbecco's modified Eagle's medium (DMEM; Thermo Fisher Scientific, Waltham, Massachusetts, USA) added with 10% fetal bovine serum (FBS; Biological Industries, Beit-Haemek, Israel) at 37 °C with 5% CO_2. EV71 and coxsackieviruses B3 (CVB3) and ECO11 were obtained from State Key Laboratory of Virology, Wuhan Institute of Virology, Chinese Academy of Sciences; Coxsackieviruses B4-5 (CVB4-5), and B4-7 (CVB4-7) were obtained from Key Laboratory of Etiology and Epidemiology of Emerging Infectious Diseases in Universities of Shandong. A small-molecule library was purchased from Selleck Chemicals (No. L1700, Houston, Texas, USA). Ribavirin was purchased from Sichuan Kelun Pharmaceutical Co. (Sichuan, China). An anti-EV71 VP1 antibody and a rabbit anti-dsRNA antibody were purchased from Abcam (Cambridge, UK) and Scions (Jacques Chirac, Hungary), respectively. Polyclonal phosphorylation antibodies of C-RAF, MEK, and ERK1/2 and anti-C-RAF, anti-MEK, and anti-ERK1/2 antibodies were purchased from Cell Signaling Technology (Boston, USA) and Proteintech Group (Chicago, Illinois, USA).

2.2. High-throughput screening

A high-throughput screening assay based on the cytopathic effect (CPE) was performed as previously reported (Wang et al., 2022). RD cells were infected with EV71 at a multiplicity of infection (MOI) of 0.1 for 2 h and were treated with the small-molecule library compounds (6000 compounds) at 10,000 nmol/L for 20 h. Observation of CPE was conducted under the optical microscope.

2.3. MTT assay

Cytotoxicity was determined by the MTT assay. Cells cultured in 96-well plates were treated with serially diluted compounds. After 48 h, the culture supernatant was removed and 0.5 mg/mL MTT was added. The cells were further incubated at 37 °C for 4 h. Dimethyl sulfoxide (DMSO) was added to dissolve the formazan crystals formed and the absorbance of the formazan crystals was examined using a microplate reader at 490 nm (TECAN, Swiss). The 50% cytotoxic concentration (CC_{50}) was determined using absorbance.

2.4. Plaque assay

For virus quantification, plaque assays were performed as described previously (Wang et al., 2022). Shortly, Vero cells were seeded in 6-well plates and cultured for 20 h. The cells were infected with viruses diluted in DMEM containing 2% FBS for 2 h, then covered with DMEM containing 0.8% low melting-point agarose (No. 2276GR005; BioFroxx GmbH) and 2% FBS at 37 °C for 48 h. After paraformaldehyde fixation, the samples were stained with 0.5% crystal violet. Then, the number of plaques was calculated.

2.5. Immunofluorescence staining

RD cells were cultured in 24-well plates. After infection with EV71 (MOI = 0.1) for 2 h, RD cells were treated with PLX8394 for 20 h. After paraformaldehyde fixation, the RD cells were permeabilized with 0.5% Triton X-100 and closed with phosphate-buffered saline (PBS) supplemented with 5% BSA for 1 h. Then, the RD cells were incubated with double-stranded RNA (dsRNA) antibody at 4 °C for 20 h. Next, the RD cells were incubated with CY3-labeled secondary antibody (Cat: SA00009-1, Proteintech, Chicago, Illinois, USA) for 1 h and then incubated with DAPI (Thermo Fisher Scientific, Waltham, Massachusetts, USA) at 37 °C for 10 min. Finally, immunofluorescence images were obtained using the Operetta CLS High-Content Analysis System (PerkinElmer, Waltham, Massachusetts, USA).

2.6. RT-qPCR

Total RNA was collected from cells using the Ultrapure RNA Kit (No. CWO581 M; CWBIOTECH, Beijing, China) following the manufacturer's instructions. cDNA was synthesized using reverse transcriptase (Promega, Madison, WI, USA). Relative viral VP1 RNA levels were determined by RT-qPCR, using *GAPDH* as an internal reference. The primers used for RT-qPCR are listed in Supplementary Table S1.

2.7. Western blot analysis

The Western blot analysis was performed as previously reported (Yang et al., 2019). Shortly, polyclonal phosphorylation antibodies of C-RAF, MEK, ERK1/2, and anti-C-RAF, anti-MEK, and anti-ERK1/2 antibodies, and monoclonal anti-EV71 VP1 and anti-GAPDH antibodies were diluted 1:1000 in primary antibody dilution buffer (No. BL506A; Biosharp, Hefei, China). Corresponding secondary antibodies were diluted at 1:5000 in PBST (PBS added with 0.05% Tween 20) containing 2% skim milk. Chemiluminescence was used to visualize the proteins and images were acquired using the Signal West Pico Chemiluminescent Substrate (Bio Rad, Hercules, California, USA).

2.8. Time-of addition assay

For post entry step assay, RD cells were cultured in 12-well plates and infected with EV71 (MOI = 0.1) for 2 h at 37 °C, then cells were washed with DMEM. Next, serial diluted PLX8394 (0, 32, 160, 800, 4000, 20000 nmol/L) were incubated with RD cells for 20 h. Viral mRNA levels were detected by RT-qPCR and IC_{50} was calculated using the inhibition rate at RNA level.

For early entry step assay, RD cells were pretreated with PLX8394 for 2 h at 37 °C, then washed with DMEM. Next, EV71 at an MOI of 0.1 was incubated with cells for 2 h and then washed with DMEM, and next cultured for 20 h. Relative viral VP1 RNA levels were detected by RT-qPCR and IC_{50} was calculated using the inhibition rate at RNA level.

To test the duration of PLX8394 in inhibiting EV71 replication, RD cells were cultured in 12-well plates and infected with EV71 (MOI = 0.1) for 2 h at 37 °C, and then PLX8394 or ribavirin at the concentration of 4,000 nmol/L were added to the wells. The cells were collected at 8, 12, 18, and 20 h post-treatment. VP1 protein levels were examined by Western blot and RNA levels were examined by RT-qPCR.

2.9. Antiviral activity assay

HeLa or RD cells were cultured in 12-well plates and infected with EV71, CVB3, CVB4-5, CVB4-7 or ECHO11 at a MOI of 0.1. PLX8394 was dissolved in DMSO and diluted in 2% FBS, and ribavirin was diluted in 2% FBS. At 2 h post-infection, a dilution series of PLX8394 and ribavirin were added to the wells. After cultivation for 20 h, total RNA was collected from the cells for RT-qPCR. The 50% maximal inhibitory concentration (IC_{50}) was calculated using the inhibition rate at the RNA level. The CC_{50} value was determined using an MTT assay. The selective index (SI) was determined as the ratio of CC_{50} to IC_{50}.

2.10. Animal experiment

The animal experiments were carried out under the approval of the Animal Care and Use Committee of the Wuhan Institute of Virology (WIVA38202103). Pregnant ICR mice were purchased from Beijing Vital River Laboratory Animal Technology (Beijing, China). Animal assays were divided into two parts, the survival rate experiment and the tissue-collection experiment. In the survival rate experiment, suckling mice were divided into three groups (n = 12/group), the "normal control", "non-treatment" and "treatment" groups. The "normal control" mice group was uninfected with EV71. In the "non-treatment" and "treatment" groups, three-day-old suckling mice were infected with EV71 at 8×10^6 plaque-forming units (PFU)/mouse by intraperitoneal injection. To determine the protective effect of PLX8394 in mice, PLX8394 or placebo (5% DMSO, 5% Tween-80, 40% PEG-300, and 50% double distilled water) was injected into the abdominal cavity of "treatment" and "non-treatment" mice groups respectively, at a concentration of 5 mg/kg once a day for 8 days, starting at the time of infection. In the tissue-collection experiment (n = 5–6/group), all three groups of mice were sacrificed on day 2 post-treatment, and relative viral RNA levels in the heart and liver were determined by RT-qPCR. In addition, heart and liver tissues were stained with hematoxylin and eosin (HE) to observe pathological changes (Cáceres et al., 2021).

2.11. Statistical analysis

GraphPad Prism software was subject to statistical analysis. All data are displayed as mean ± standard error of triplicate determinations. Data difference analysis was conducted using *Student's* t-test. The *P* values < 0.05 (*), <0.01 (**), <0.001 (***) and ns were considered significant, very significant, extremely significant, and non-significant respectively.

3. Results

3.1. Identification of potent and low-toxicity compounds that block EV71

EV71-infected RD cells were treated with 6000 small compounds at the concentration of 10,000 nmol/L, and the potential antiviral activity of the compounds was determined based on the CPE. Potential antiviral compounds were scored ranging from "-" (no cytopathic changes) to "++++" (100% cytopathic changes). Following the standard, we screened out PLX8394 (Fig. 1A), a RAF inhibitor, which significantly relieved the CPE induced by EV71 and showed antiviral activity. Subsequently, we explored the relationship between PLX8394 doses and the CPE. The results showed that the CPE decreased with increasing concentration of PLX8394 and was even completely abrogated when the PLX8394 concentration was increased to 4000 nmol/L (Fig. 1B). Next, we used the MTT assay to evaluate the cytotoxicity of PLX8394 on RD and HeLa cells, using ribavirin as the positive control (Fig. 1C–F). The CC_{50} values of PLX8394 in RD and HeLa cells were 19,075 and 37,523 nmol/L, respectively, and those of ribavirin were 46,100 and 123,100 nmol/L, respectively. It demonstrated that PLX8394 was an effective antiviral agent against EV71 infection within the safe concentration.

3.2. PLX8394 presents high anti-EV71 activity

We further examined the antiviral activity of PLX8394 by treating EV71-infected cells with serially diluted PLX8394, using ribavirin as a positive control. RT-qPCR and Western blot were applied to evaluate EV71 RNA and its structural protein VP1 expression, respectively (Fig. 2A and B). Results indicated that EV71 replication was inhibited by PLX8394 in a dose-dependent manner. PLX8394 was superior to ribavirin in suppressing viral RNA levels. At the concentration of 4000 nmol/L, the inhibition rate was nearly 99% for PLX8394, whereas it was only 30% for
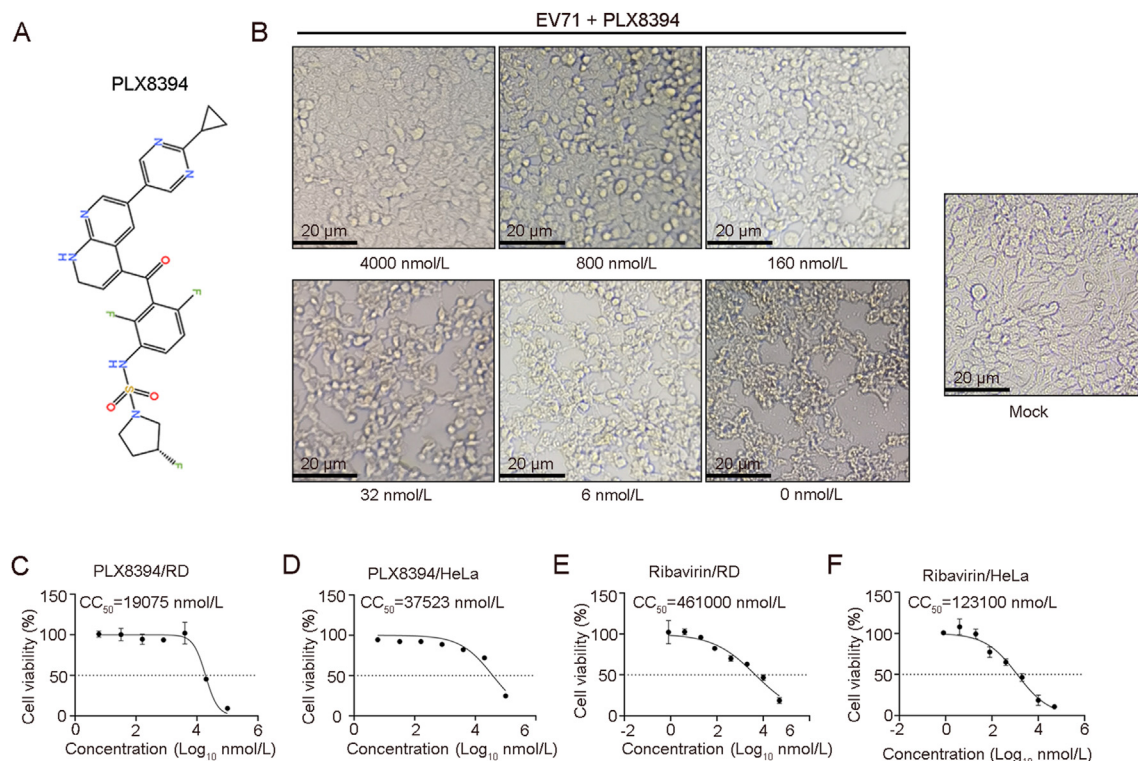

Fig. 1. Discovery of potent and low-toxicity active compounds that block EV71 infection. **A** Structure of PLX8394. **B** After infection with EV71 (MOI = 0.1) for 2 h, infected-RD cells were treated with PLX8394 for 48 h. Images of the CPE were acquired using an optical microscope. **C–F** RD or HeLa cells were incubated with serially diluted PLX8394 or ribavirin for 48 h. Cytotoxicity was assessed using the MTT assay. CC_{50} values of PLX8394 in RD and HeLa cells were 19,075 and 37,523 nmol/L, respectively (**C–D**). CC_{50} values of ribavirin in RD and HeLa cells were 461,000 and 123,100 nmol/L, respectively (**E–F**). All experiments were independently repeated three times.
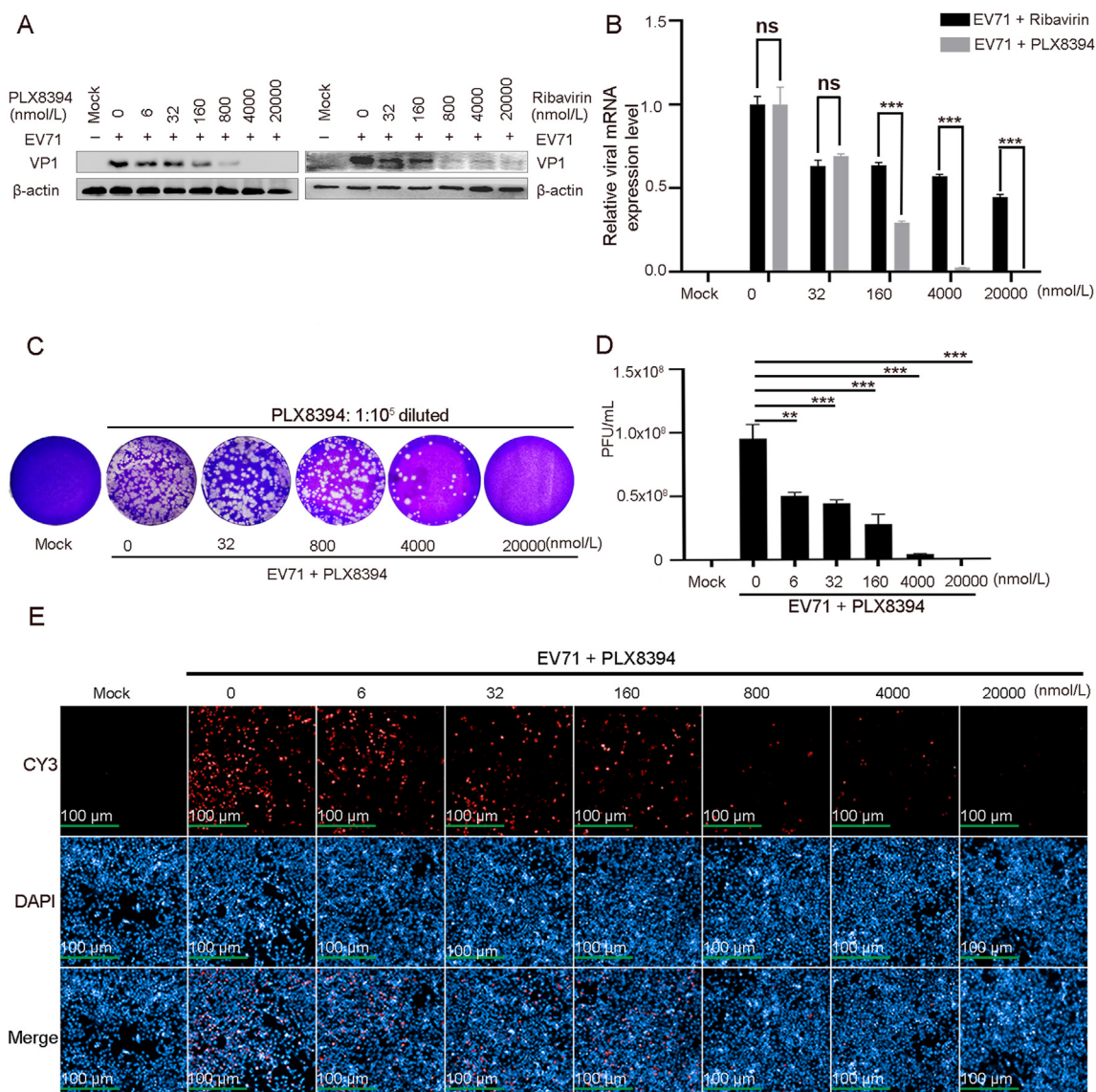
Fig. 2. Antiviral effect of PLX8394 *in vitro*. **A–B** After infection with EV71 (MOI = 0.1) for 2 h, RD cells were treated with PLX8394 or ribavirin for 20 h. VP1 protein levels were examined by Western blot analysis (**A**). Viral RNA levels relative to *GADPH* levels were detected by RT-qPCR (**B**). **C–D** The treated RD cells and culture medium were freeze-thawed three times and the number of infective clones of EV71 was determined by the plaque assay (**C**). Quantitative data of the plaque assay (**D**). (**E**) Immunofluorescence staining evaluation of the antiviral effect of PLX8394. dsRNA of EV71 is labeled with red fluorescence (CY3), nuclei are labeled with blue fluorescence (DAPI). *$P < 0.05$, **$P < 0.01$, ***$P < 0.001$. All experiments were independently repeated three times.

ribavirin (Fig. 2B). The antiviral effect of PLX8394 was also observed using the plaque assay (Fig. 2C); the number of infectious virus particles gradually decreased with increasing PLX8394 concentration (Fig. 2D).

To further demonstrate the antiviral activity of PLX8394 against EV71, we performed an immunofluorescence assay to visualize the antiviral effect. As shown in Fig. 2E, the dsRNA of EV71 was marked with red fluorescence (CY3) and nuclei were marked with blue fluorescence (DAPI). The red fluorescence was gradually inhibited with increasing concentrations of PLX8394. These results indicate that PLX8394 was more effective than ribavirin against EV71 infection *in vitro*.

3.3. PLX8394 affects the post-entry phase of EV71 and duration of PLX8394 efficacy

We evaluated which stage of the virus life cycle is affected by PLX8394. First, to verify whether PLX8394 affects the post-entry phase (Fig. 3A), EV71-infected RD cells were treated with different concentrations of PLX8394 for 20 h at 2 h post infection. It showed that PLX8394

exhibited antiviral activity, with the lower IC_{50} and higher SI values ($IC_{50} = 75.5$ nmol/L, SI = 252.6), which suggested that PLX8394 affects intracellular viral proliferation (Fig. 3B and C). Then, to verify whether PLX8394 affects virus entry phase (Fig. 3D), RD cells were pre-treated with PLX8394 for 2 h before infection with EV71. Then PLX8394 pre-treated RD cells were incubated with EV71 (MOI = 0.1) for 2 h, and finally the cells were washed with DMEM and cultured for 20 h before testing viral RNA levels. The results in Fig. 3E and F showed that the viral RNA level was gradually inhibited with increasing PLX8394 concentration, indicating that PLX8394 may prevent EV71 entry in RD cells to a certain degree. However, the antiviral effect was lower than that exhibited in the post-entry experiment, which indicates that PLX8394 mainly acts on intracellular viral proliferation.

To investigate the duration of PLX8394 in inhibiting EV71 replication, we evaluated the antiviral effect at four time points (8, 12, 16, and 20 h), using ribavirin as a positive control. According to the results shown in Fig. 3G and H, at 4000 nmol/L, PLX8394 was obviously superior to ribavirin in decreasing viral RNA and VP1 protein levels. Notably,
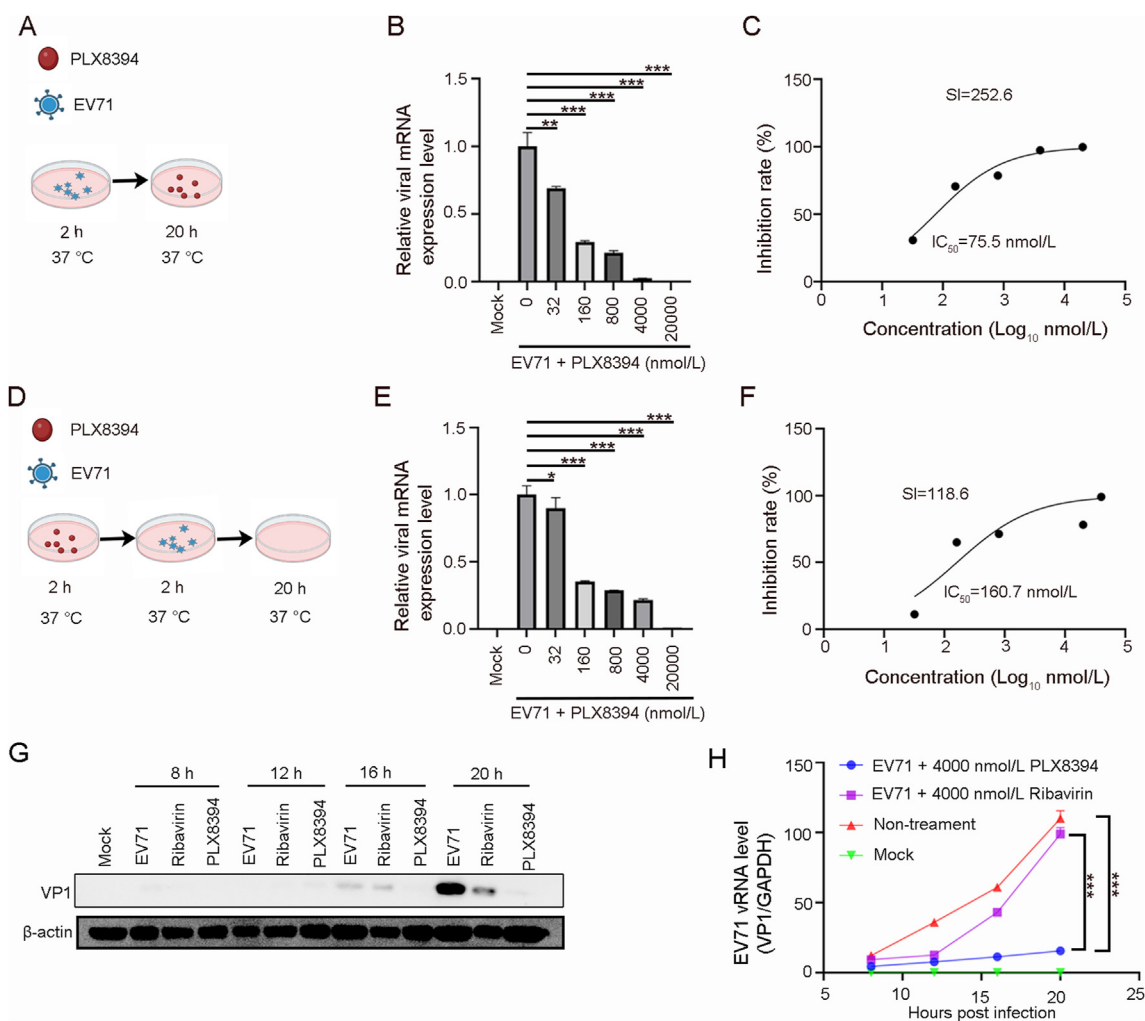
Fig. 3. PLX8394 targets EV71 at the phase of post-entry, and the inhibition can last for 20 h. **A–C** After infection with EV71 (MOI = 0.1) for 2 h, RD cells were treated with PLX8394 for 20 h. RNA levels were tested by RT-qPCR. **D–F** RD cells were treated with serially diluted PLX8394 for 2 h. Then, the suspension was removed and the cells were infected with EV71 (MOI = 0.1) for 2 h and cultured for 20 h. RNA levels were examined by RT-qPCR (**B, E**), and IC$_{50}$ values were calculated as the inhibition rate of viral RNA levels, and SI values were calculated as CC$_{50}$/IC$_{50}$ (**C, F**). **G–H** After infection with EV71 (MOI = 0.1) for 2 h, the infected-RD cells were treated with PLX8394 or ribavirin at a concentration of 4000 nmol/L for 20 h. VP1 protein levels at 8, 12, 16, and 20 h were examined by Western blot (**G**) and RNA levels at 8, 12, 16, and 20 h were examined by RT-qPCR (**H**). *$P < 0.05$, **$P < 0.01$, ***$P < 0.001$. All experiments were independently repeated three times.

compared with ribavirin, PLX8394 still showed effective antiviral activity at 20 h after treatment. These results suggest that the antiviral effect of PLX8394 may depend on inhibiting EV71 proliferation, which can last for at least 20 h, and the inhibition effect of PLX8394 is superior to that of ribavirin.

3.4. PLX8394 inhibits EV71 replication by blocking the RAF/MEK/ERK signaling pathway

To evaluate the involvement of RAF/MEK/ERK in EV71 replication, we assessed changes of the RAF/MEK/ERK signaling pathway in EV71-infected RD cells by Western blot. According to the result shown in Fig. 4A, the VP1 protein level increased with increasing EV71 titers, which is consistent with the same trend of the phosphorylation degree of C-RAF, MEK, and ERK. This trend was also observed in a time-dependent experiment. As shown in Fig. 4B, VP1 protein levels and phosphorylation degree of C-RAF, MEK, and ERK were positively correlated with the duration of EV71 infection, indicating that the longer the infection, the greater the amount of virus and the stronger the activation of the RAF/MEK/RAF signaling pathway. These results suggest that the host RAF/MEK/ERK pathway is activated during EV71 replication.

PLX8394 is a RAF inhibitor, thus we examined the influence of PLX8394 on the RAF/MEK/ERK pathway. It showed that the phosphorylation degree of C-RAF, MEK, and ERK in RD cells gradually decreased with increasing concentrations of PLX8394 (Fig. 4C). To investigate whether inhibition of the activation of the RAF/MEK/ERK pathway by PLX8394 could attenuate EV71 replication, we measured the influence of PLX8394 on VP1 expression by altering the level of RAF/MEK/RAF pathway activation in EV71-infected RD cells. With increasing concentrations of PLX8394, the RAF/MEK/ERK signaling pathway activated by EV71, and VP1 protein levels gradually decreased (Fig. 4D). These results suggest that the activation of the host RAF/MEK/ERK pathway plays a crucial part in EV71 replication, and PLX8394 inhibits EV71 replication by blocking the RAF/MEK/ERK pathway.

3.5. PLX8394 presents broad-spectrum antiviral activity

As many viruses rely on host RAF/MEK/ERK pathway for replication, we speculate that PLX8394 may possess broad-spectrum activity. Therefore, we assessed the antiviral activity of PLX8394 against several enteroviruses, including CVB3, CVB4-5, CVB4-7, and ECHO11. PLX8394 exhibited effective antiviral activity against selected viruses. As shown in Fig. 5A–D, PLX8394 inhibited the replication of CVB3, CVB4-5, CVB4-7,
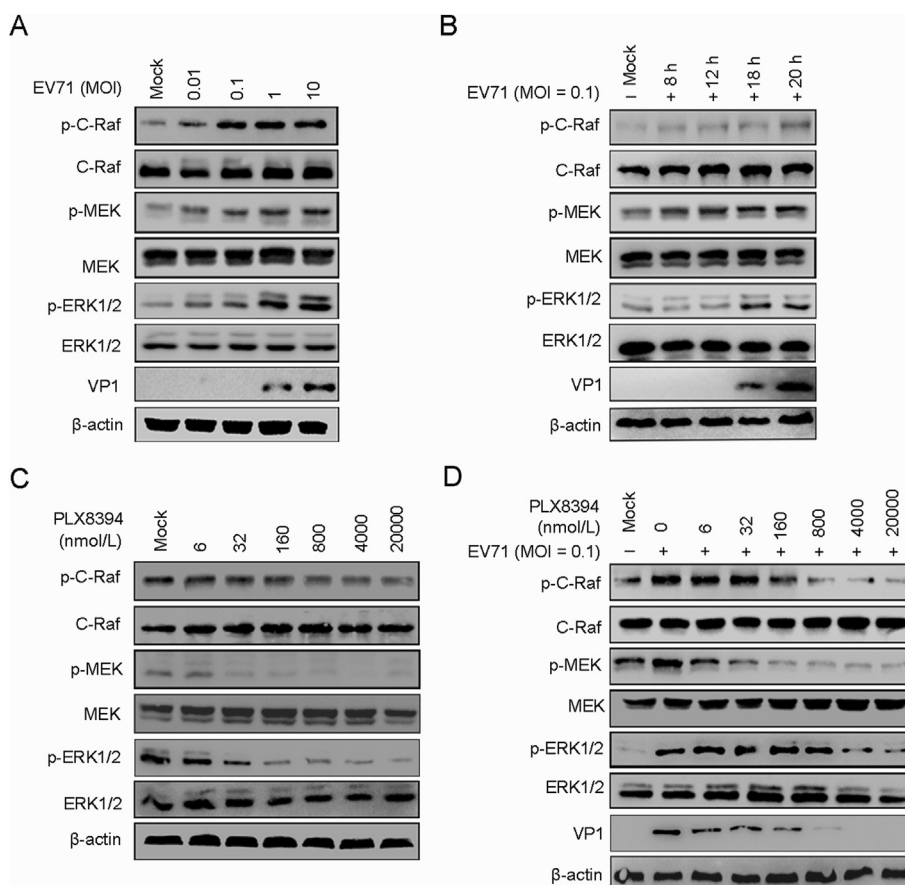
Fig. 4. PLX8394 inhibits EV71 replication by blocking the RAF/MEK/ERK signaling pathway. **A** RD cells were infected with EV71 at an MOI of 0.01, 0.1, 1, or 10 for 2 h. After removing the suspension, the cells were further cultured for 12 h. VP1, C-RAF, MEK, and ERK protein levels and the phosphorylation levels of C-RAF, MEK, and ERK were analyzed by Western blot. **B** After infection with EV71 (MOI = 0.1) for 2 h, and then removal of the suspension, the cells were collected at 8, 12, 18, and 20 h. VP1, C-RAF, MEK, and ERK proteins levels and the phosphorylation levels of C-RAF, MEK, and ERK were analyzed by Western blot. **C** RD cells were treated with serially diluted PLX8394 for 20 h and C-RAF, MEK, and ERK proteins levels and the phosphorylation levels of C-RAF, MEK, and ERK were examined by Western blot. β-actin was used as a loading control. **D** After infection with EV71 (MOI = 0.1) for 2 h, the cells were treated with different concentrations of PLX8394 for 20 h. VP1, C-RAF, MEK, and ERK proteins levels and the phosphorylation levels of C-RAF, MEK, and ERK were examined by Western blot. All experiments were independently repeated three times.

and ECHO11 in a dose-dependent manner with the IC_{50} values of 44.1, 58.4, 42.9, and 126.1 nmol/L (Fig. 5E), respectively. Notably, PLX8394 was more effective against CVB4-7 and ECHO11 than the other viruses. At the concentration of 20,000 nmol/L, no viral load was detected. Thus, PLX8394 may be a broad-spectrum antiviral compound against enteroviruses infection.

3.6. PLX8394 exhibits antiviral activity in suckling mice

Given the anti-EV71 effect of PLX8394 *in vitro*, we next examined the antiviral activity of PLX8394 in a suckling mouse model (Fig. 6A). Three-day-old suckling mice were intraperitoneally injected with EV71 at 8×10^6 PFU/mouse and treated with PLX8394 or placebo once a day for 8 days. In the "non-treatment" group (treated with placebo), mice began to die as of 2 days post-infection and all were dead by 5 days post-infection. In contrast, treatment with PLX8394 provided approximately 70% protection to infected suckling mice on day 8 (Fig. 6B). To further evaluate the antiviral effect of PLX8394 *in vivo*, we detected viral RNA levels in mouse tissues. Heart and liver tissues were collected on day 2 post-infection and viral RNA levels were determined by RT-qPCR (Fig. 6C and D). Small amounts of viral RNA were detected in heart tissues, which may account for the severe complications caused by EV71. Virus loads in liver tissues were higher than those in heart tissues. EV71 loads in the

livers and hearts were substantially lower in the PLX8394 treatment group than in the non-treatment group.

Finally, liver and heart tissues collected on day 2 post-infection were stained with HE. As shown in Fig. 6E, no abnormality was found in the "normal control" group, however, considerable inflammatory cells had infiltrated the liver and a small number of liver cells had undergone apoptosis in the "non-treatment" group. In the heart tissues, only a few inflammatory cells and limited apoptosis were observed. The liver inflammatory reaction was abrogated by PLX8394 treatment, and no inflammatory cells were observed in the hearts of mice in the PLX8394 treatment group. Thus, PLX8394 exerts an antiviral effect and relieves inflammation *in vivo*.

4. Discussion

In past decades, EV71 infection outbroke sporadically worldwide, resulting in the death of a few children and infants due to severe neurological complications. However, there are no specific medicines for the treatment of EV71 infection; therefore, we urgently need new medicines to treat diseases caused by EV71 infection (Abzug, 2014; Yi et al., 2017; Zhang et al., 2021). As drug discovery is time-consuming and expensive, repurposing conventional drugs is a promising approach. PLX8394, a RAF inhibitor, is being tested in clinical trials for
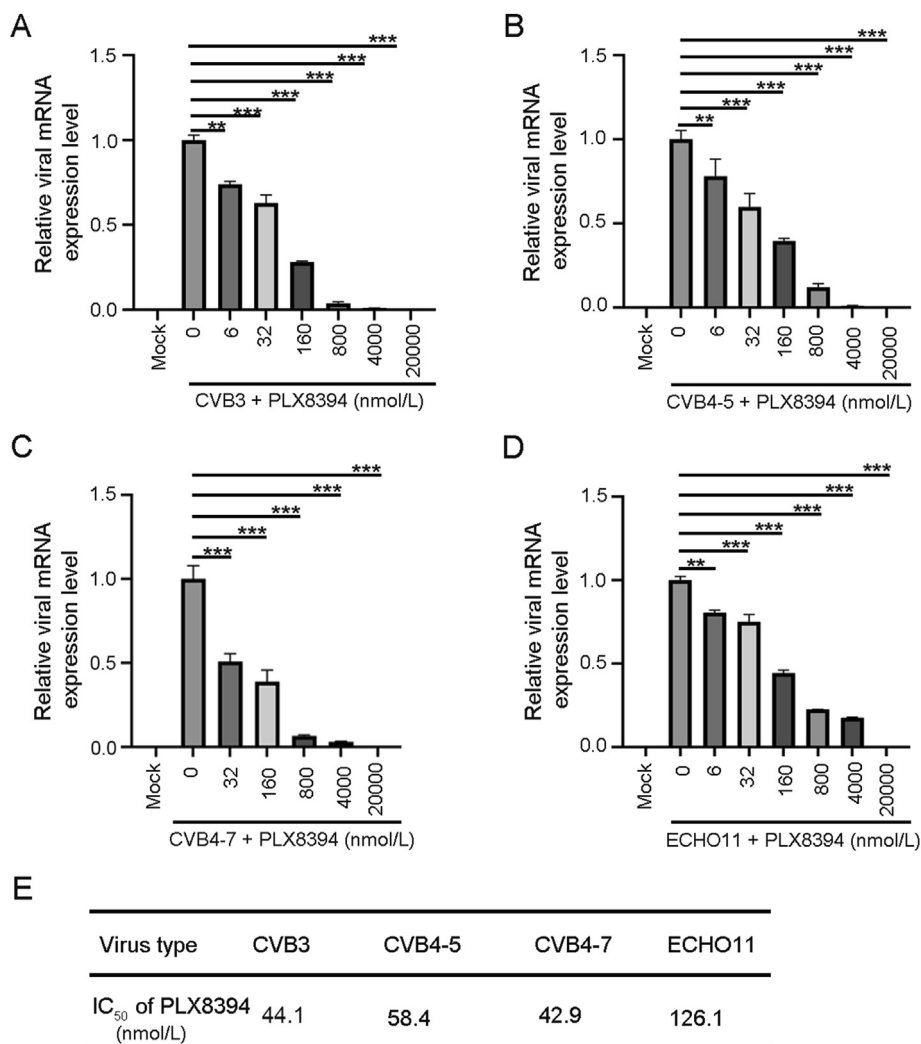
Fig. 5. PLX8394 exhibits broad-spectrum antiviral activity against enteroviruses. HeLa cells were infected with CVB3 (**A**), CVB4-5 (**B**), CVB4-7 (**C**), or ECHO11 (**D**) at an MOI of 0.1 for 2 h and then treated with serially diluted PLX8394 for 20 h. Viral RNA levels were detected by RT-qPCR. **E** The IC_{50} values of PLX8394 against selected enteroviruses were determined in experiments described above. $*P < 0.05$, $**P < 0.01$, $***P < 0.001$. All experiments were independently repeated three times.

the treatment of advanced unresectable solid tumors according to the information in the U.S. National Library of Medicine. Here, we first reveal that PLX8394 has a strong antiviral activity, superior to that of the traditional drug ribavirin against EV71. Meanwhile, PLX8394 can sustain an efficient antiviral activity for 20 h, which is better than ribavirin. More notably, PLX8394 exhibits antiviral activity *in vivo*, providing a 70% survival rate in infected-EV71 suckling mice, reducing the viral load, and suppressing the inflammatory response in the livers and hearts of mice infected by EV71. Given the novel discovery, it is reasonable to consider PLX8394 as a short-term application to treat acute EV71 infection.

The antiviral activity mechanism of PLX8394 is unclear. Therefore, we investigated which phase in virus life cycle targeted by PLX8394. Our data indicated that PLX8394 is more efficient in viral post-entry phase. These results show that PLX8394 mainly acts on intracellular viral proliferation. PLX8394 is a new RAF inhibitor, which belongs to the RAF/MEK/ERK signaling pathway. Studies have reported that this signaling pathway is stimulated upon EV71 infection and essential for EV71 infection (Tung et al., 2010; Bian et al., 2015; Wen et al., 2015). It is feasible to speculate that PLX8394 targets the host's RAF/MEK/ERK signaling pathway to inhibit viral proliferation. Our results showed that PLX8394 blocked the RAF/MEK/ERK pathway in non-infected cells by inhibiting the phosphorylation of C-RAF. More importantly,

RAF/MEK/ERK pathway activation by EV71 is inhibited by PLX8394 treatment. These data indicate that PLX8394 may inhibit EV71 replication by blocking the host RAF/MEK/ERK signaling pathway.

Aiming at the host factors has many advantages compared with direct-acting antiviral agents. One major advantage is that it confers broad-spectrum antiviral activity (Ji and Li, 2020). One host protein or signaling pathway can play a role in the lifecycle of multiple viruses and thus, specific inhibitors may have broad-spectrum antiviral activity. The MAPK pathway is used by a wide variety of viruses, including hepatitis B virus, influenza A virus, Newcastle disease virus, human immunodeficiency virus 1, and enteroviruses (Benn and Schneider, 1994; Flory et al., 1998; Huber et al., 1999; Pleschka et al., 2001; Ludwig et al., 2004; Yin et al., 2015). Therefore, it is reasonable for PLX8394, a RAF inhibitor belonging to the MAPK family, to confer broad-spectrum antiviral activity. Besides EV71, we found that PLX8394 is effective against other enteroviruses, including CBV3, CVB4-5, CVB4-7, and EHCO11. Importantly, host-targeting antiviral agents may be effective against emerging viruses that use the same host factors for replication (Ji and Li, 2020). Evidence indicates that SARS-CoV-2 activates the RAF/MEK/ERK pathway, and MAPK inhibitors and knockdown of MEK and ERK interfered with SARS-CoV-2 replication. Thus, PLX8394 may be a candidate for the treatment of SARS-CoV-2 infection (Ghasemnejad-Berenji and Pashapour, 2021).
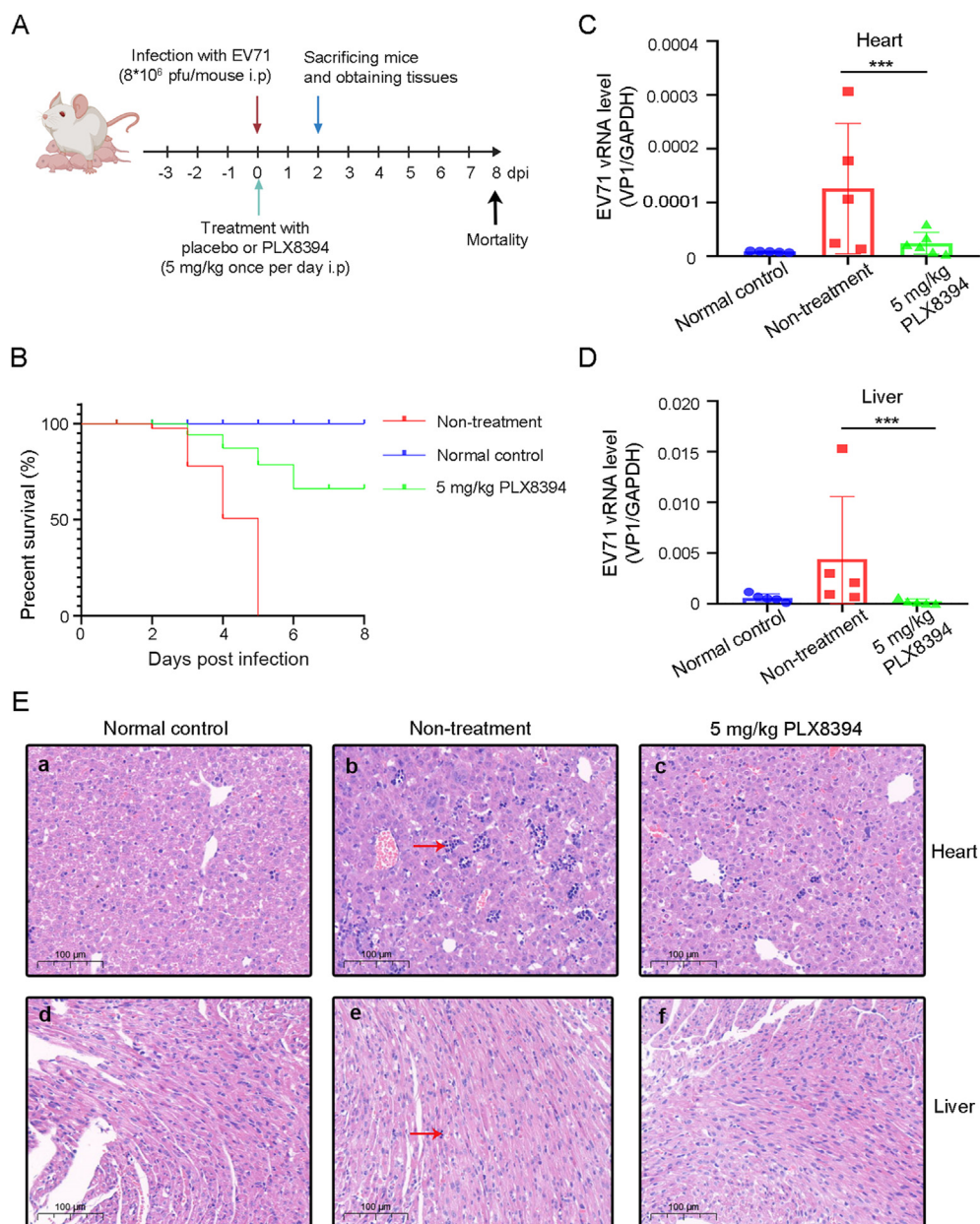
Fig. 6. PLX8394 exerts anti-EV71 activity *in vivo*. **A** Diagram of the animal experiment. Three-day-old suckling ICR mice were infected with EV71 at 10^6 PFU and treated with PLX8394 at 5 mg/kg or placebo over the following 8 days. **B** The survival rate was monitored daily until 8 days post-infection. **C–D** Heart and liver tissues from mice in the "normal control," "non-treatment," and "treatment" groups were collected on day 2 post-infection and viral RNA levels were analyzed by RT-qPCR. **E** The tissues were stained with HE to reveal pathological changes. $*P < 0.05$, $**P < 0.01$, $***P < 0.001$. All experiments were independently repeated three times.

However, targeting a host factor is likely to result in toxicity issues as the target protein is probably necessary for the normal functioning of the cell. This is not true for all target proteins, though, because some of them are unnecessary for cell function but necessary for the viral life cycle. Moreover, toxicity can be avoided by changing the construction of chemical compounds and shortening treatment time. As for PLX8394, the concentration necessary for effective antiviral activity is non-cytotoxic, and the IC_{50} values are much lower than the CC_{50} values in RD and HeLa cells. Therefore, a safe treatment window for the application of PLX8394 can be established. A short-term application to treat acute EV71 infection is also possible. Furthermore, if the PLX8394 structure can be modified to improve the antiviral activity and reduce toxicity, this compound may have further application for EV71 infection treatment and lay a foundation for the development of new drugs against EV71.

5. Conclusions

This research showed that PLX8394 presents highly effective antiviral activity against EV71 *in vivo* and *in vitro*. The broad-spectrum antiviral activity and time-dependent and mechanism data indicate that PLX8394 is a potential antiviral drug.

Data availability

Data are available within the article or its supplementary materials.

Ethics statement

The animal experiments had the approval of the Animal Care and Use Committee of the Wuhan Institute of Virology (WIVA38202103).

Author contributions

Chengyuan Wu: methodology, data curation and writing – original draft preparation. Guangyan Zhu: methodology, data curation and writing – original draft preparation. Fang Qiu: formal analysis and validation. Binbin Lin: formal analysis and validation. Dingyu Zhang: conceptualization, supervision and funding acquisition acquisition. Qingyu Yang: methodology, project administration. Chaolin Huang: conceptualization, project administration and supervision.

Conflict of interest

The authors declare that they have no competing interests.

Acknowledgments

Appendix A. Supplementary data

Supplementary data to this article can be found online at https://doi.org/10.1016/j.virs.2023.01.006.

References

Abzug, M.J., 2014. The enteroviruses: problems in need of treatments. J. Infect. 68 (Suppl. 1), S108–S114.

Benn, J., Schneider, R.J., 1994. Hepatitis B virus HBx protein activates Ras-GTP complex formation and establishes a Ras, Raf, MAP kinase signaling cascade. Proc. Natl. Acad. Sci. U.S.A. 91, 10350–10354.

Bian, L., Wang, Y., Liu, Q., Xia, J., Long, J.E., 2015. Prediction of signaling pathways involved in enterovirus 71 infection by algorithm analysis based on miRNA profiles and their target genes. Arch. Virol. 160, 173–182.

Bogoyevitch, M.A., Kobe, B., 2006. Uses for JNK: the many and varied substrates of the c-Jun N-terminal kinases. Microbiol. Mol. Biol. Rev. 70, 1061–1095.

Cáceres, C.J., Hu, Y., Cárdenas-García, S., Wu, X., Tan, H., Carnaccini, S., Gay, L.C., Geiger, G., Ma, C., Zhang, Q.Y., Rajao, D., Perez, D.R., Wang, J., 2021. Rational design of a deuterium-containing M2-S31N channel blocker UAWJ280 with in vivo antiviral efficacy against both oseltamivir sensitive and -resistant influenza A viruses. Emerg. Microb. Infect. 10, 1832–1848.

Chang, L.Y., Tsao, K.C., Hsia, S.H., Shih, S.R., Huang, C.G., Chan, W.K., Hsu, K.H., Fang, T.Y., Huang, Y.C., Lin, T.Y., 2004. Transmission and clinical features of enterovirus 71 infections in household contacts in Taiwan. JAMA 291, 222–227.

Chong, P., Liu, C.C., Chow, Y.H., Chou, A.H., Klein, M., 2015. Review of enterovirus 71 vaccines. Clin. Infect. Dis. 60, 797–803.

Dai, W., Xie, S., Chen, C., Choi, B.H., 2021. Ras sumoylation in cell signaling and transformation. Semin. Cancer Biol. 76, 301–309.

Flory, E., Weber, C.K., Chen, P., Hoffmeyer, A., Jassoy, C., Rapp, U.R., 1998. Plasma membrane-targeted Raf kinase activates NF-kappaB and human immunodeficiency virus type 1 replication in T lymphocytes. J. Virol. 72, 2788–2794.

Ghasemnejad-Berenji, M., Pashapour, S., 2021. SARS-CoV-2 and the possible role of Raf/MEK/ERK pathway in viral survival: is this a potential therapeutic strategy for COVID-19? Pharmacology 106, 119–122.

Han, Y., Chen, Z., Zheng, K., Li, X., Kong, J., Duan, X., Xiao, X., Guo, B., Luan, R., Long, L., 2020. Epidemiology of hand, foot, and mouth disease before and after the introduction of enterovirus 71 vaccines in chengdu, China, 2009-2018. Pediatr. Infect. Dis. J. 39, 969–978.

Huber, M., Watson, K.A., Selinka, H.C., Carthy, C.M., Klingel, K., Mcmanus, B.M., Kandolf, R., 1999. Cleavage of RasGAP and phosphorylation of mitogen-activated protein kinase in the course of coxsackievirus B3 replication. J. Virol. 73, 3587–3594.

Ji, X., Li, Z., 2020. Medicinal chemistry strategies toward host targeting antiviral agents. Med. Res. Rev. 40, 1519–1557.

Khojasteh Poor, F., Keivan, M., Ramazii, M., Ghaedrahmati, F., Anbiyaiee, A., Panahandeh, S., Khoshnam, S.E., Farzaneh, M., 2021. Mini review: the FDA-approved prescription drugs that target the MAPK signaling pathway in women with breast cancer. Breast Dis. 40, 51–62.

Leong, S.Y., Ong, B.K., Chu, J.J., 2015. The role of Misshapen NCK-related kinase (MINK), a novel Ste20 family kinase, in the IRES-mediated protein translation of human enterovirus 71. PLoS Pathog. 11, e1004686.

Ludwig, S., 2011. Disruption of virus-host cell interactions and cell signaling pathways as an anti-viral approach against influenza virus infections. Biol. Chem. 392, 837–847.

Ludwig, S., Planz, O., Pleschka, S., Wolff, T., 2003. Influenza-virus-induced signaling cascades: targets for antiviral therapy? Trends Mol. Med. 9, 46–52.

Ludwig, S., Wolff, T., Ehrhardt, C., Wurzer, W.J., Reinhardt, J., Planz, O., Pleschka, S., 2004. MEK inhibition impairs influenza B virus propagation without emergence of resistant variants. FEBS Lett. 561, 37–43.

Nagata, K., Kawaguchi, A., Naito, T., 2008. Host factors for replication and transcription of the influenza virus genome. Rev. Med. Virol. 18, 247–260.

Pei, Z., Wang, H., Zhao, Z., Chen, X., Huan, C., Zhang, W., 2022. Chemokine PF4 inhibits EV71 and CA16 infections at the entry stage. J. Virol. 96, e0043522.

Peng, H., Shi, M., Zhang, L., Li, Y., Sun, J., Zhang, L., Wang, X., Xu, X., Zhang, X., Mao, Y., Ji, Y., Jiang, J., Shi, W., 2014. Activation of JNK1/2 and p38 MAPK signaling pathways promotes enterovirus 71 infection in immature dendritic cells. BMC Microbiol 14, 147.

Pleschka, S., Wolff, T., Ehrhardt, C., Hobom, G., Planz, O., Rapp, U.R., Ludwig, S., 2001. Influenza virus propagation is impaired by inhibition of the Raf/MEK/ERK signalling cascade. Nat. Cell Biol. 3, 301–305.

Schmidt, N.J., Lennette, E.H., Ho, H.H., 1974. An apparently new enterovirus isolated from patients with disease of the central nervous system. J. Infect. Dis. 129, 304–309.

Tung, W.H., Hsieh, H.L., Yang, C.M., 2010. Enterovirus 71 induces COX-2 expression via MAPKs, NF-kappaB, and AP-1 in SK-N-SH cells: role of PGE(2) in viral replication. Cell. Signal. 22, 234–245.

Wang, J., Hu, Y., Zheng, M., 2022. Enterovirus A71 antivirals: past, present, and future. Acta Pharm. Sin. B 12, 1542–1566.

Wen, T., Xu, W., Liang, L., Li, J., Ding, X., Chen, X., Hu, J., Lv, A., Li, X., 2015. Clinical efficacy of andrographolide sulfonate in the treatment of severe hand, foot, and mouth disease (HFMD) is dependent upon inhibition of neutrophil activation. Phytother Res. 29, 1161–1167.

Xu, N., Yang, J., Zheng, B., Zhang, Y., Cao, Y., Huan, C., Wang, S., Chang, J., Zhang, W., 2020. The pyrimidine analog FNC potently inhibits the replication of multiple enteroviruses. J. Virol. 94, e00204–20.

Yang, Q., Zhang, Q., Zhang, X., You, L., Wang, W., Liu, W., Han, Y., Ma, C., Xu, W., Chen, J., Yang, H., Wan, P., Zhou, Y., Liu, Y., Wu, K., Yang, Z., Wu, J., 2019. HoxA10 facilitates SHP-1-Catalyzed dephosphorylation of p38 MAPK/STAT3 to Repress hepatitis B virus replication by a feedback regulatory mechanism. J. Virol. 93, e01607–18.

Yao, Z., Gao, Y., Su, W., Yaeger, R., Tao, J., Na, N., Zhang, Y., Zhang, C., Rymar, A., Tao, A., Timaul, N.M., Mcgriskin, R., Outmezguine, N.A., Zhao, H., Chang, Q., Qeriqi, B., Barbacid, M., De Stanchina, E., Hyman, D.M., Bollag, G., Rosen, N., 2019. RAF inhibitor PLX8394 selectively disrupts BRAF dimers and RAS-independent BRAF-mutant-driven signaling. Nat. Med. 25, 284–291.

Yee, P.T.I., Laa Poh, C., 2017. Impact of genetic changes, pathogenicity and antigenicity on Enterovirus- A71 vaccine development. Virology 506, 121–129.

Yi, E.J., Shin, Y.J., Kim, J.H., Kim, T.G., Chang, S.Y., 2017. Enterovirus 71 infection and vaccines. Clin. Exp. Vaccine Res. 6, 4–14.

Yin, R., Liu, X., Bi, Y., Xie, G., Zhang, P., Meng, X., Ai, L., Xu, R., Sun, Y., Stoeger, T., Ding, Z., 2015. Expression of Raf kinase inhibitor protein is downregulated in response to Newcastle disease virus infection to promote viral replication. J. Gen. Virol. 96, 2579–2586.

Yip, C.C., Lau, S.K., Woo, P.C., Yuen, K.Y., 2013. Human enterovirus 71 epidemics: what's next? Emerg. Health Threats J. 6, 19780.

Zhang, L., Chen, X., Shi, Y., Zhou, B., Du, C., Liu, Y., Han, S., Yin, J., Peng, B., He, X., Liu, W., 2014. miR-27a suppresses EV71 replication by directly targeting EGFR. Virus Gene. 49, 373–382.

Zhang, L., Wei, M., Jin, P., Li, J., Zhu, F., 2021. An evaluation of a test-negative design for EV-71 vaccine from a randomized controlled trial. Hum. Vaccines Immunother. 17, 2101–2106.